

Modelling antenna vibrations using the Signal-to-Noise Ratio (SNR) of GNSS signals

Ioulia Peppas, Panos Psimoulis, Xiaolin Meng

Nottingham Geospatial Institute, The University of Nottingham, UK

Ioulia.Peppas@nottingham.ac.uk; Panagiotis.Psimoulis@nottingham.ac.uk; Xiaolin.Meng@nottingham.ac.uk

Keywords: *SNR; multipath; monitoring; GNSS-R; antenna vibration; displacement;*

ABSTRACT

The multipath effect in GNSS measurements remains one of the dominant error sources in GNSS monitoring applications. The site-dependent, fast-changing characteristics of multipath render it difficult to model or predict, introducing errors in GNSS measurements. Current techniques to mitigate the impact of multipath effect focus mainly on repeating GNSS measurements to detect multipath-induced patterns or integrating GNSS with other sensors. However, the multipath effect is used to identify potential changes in the environment in geoscience applications, such as detecting vegetation growth, snow and tidal changes. These applications are based on the concept that for static GNSS antenna, variations in the Signal-to-Noise Ratio (SNR) measurements, induced by the multipath effect during the satellite orbit, express changes in the multipath geometry attributed to different factors (vegetation, tides, snow). In the current paper, we develop the same concept for an oscillating GNSS antenna focusing on the changes in the multipath geometry caused by the antenna rather than the satellite motion. In this study, we investigate the potential of modelling the SNR data of satellite signals and estimating reflection parameters (reflection intensity, antenna-reflector distance, reflector's tilt) and the motion characteristics (amplitude, frequency and phase of motion). The theoretical SNR model is developed and applied on simulated GNSS records for antenna oscillations in the vertical direction and horizontal reflection surface in different cases of multipath intensity and antenna motion. The validity of the model is examined using vertical controlled oscillations of GNSS antenna, executed on the roof of Nottingham Geospatial Institute, in the UK.

I. INTRODUCTION

GNSS technology is one of the recent tools applied successfully in structural monitoring, thanks to its capacity to monitor high-frequency motion (greater than 3-4 Hz) of structures and provide an accurate estimation of the structure response in an independent coordinate system, even in real-time (Moschas and Stiros, 2011). Furthermore, GNSS can identify low-frequency motion and semi-static displacement, which cannot be identified by accelerometers (Li *et al.*, 2006), and recover errors of accelerometers records due to tilt, rotation, etc. (Psimoulis *et al.*, 2015).

However, one of the major error sources in high-accuracy GNSS positioning is multipath. The multipath effect occurs when satellite signals reflected from objects around the antenna interfere with direct signals from the satellites. In combination with poor satellite geometry or shadowing of the direct signal, the multipath-induced errors can gravely impede the use of GNSS technology in some applications.

Several studies have been focusing on the multipath mitigation in urban, rural and off-shore environments involving receiver and antenna based mitigation techniques, and signal processing techniques. SNR-based phase multipath estimation and mitigation techniques (Lau and Cross, 2007; Strode and Groves, 2016) use the multipath effect on the signal-to-noise ratio of the GNSS signal to estimate the multipath

intensity and characteristics and subsequently, mitigate the related code and carrier phase errors.

The signal-to-noise ratio (SNR) is the ratio of the signal power to the noise power and is routinely measured by GNSS receivers to indicate the signal strength of the received satellite signal and the noise density (i.e., the antenna and receiver noise temperature). A less common use of the SNR is as a multipath indicator; since SNR derives from the carrier tracking loop outputs, any distortion of the correlation function due to constructive or destructive multipath interference will have an immediate effect on the measured SNR values.

Especially in structural monitoring applications, where cm-level oscillations are of interest, multipath is a dominant error source due to the abundance of potential reflectors in the surrounding of the GNSS antenna (e.g., structural elements, passing vehicles, etc.). Common signal processing multipath mitigation techniques involve the integration of GNSS with other sensors, e.g. accelerometers (Meng, Dodson and Roberts, 2007) and Robotic Total Stations (Moschas, Psimoulis and Stiros, 2013), and filtering out the low-frequency noise, which usually coincides with the multipath frequency band (Roberts *et al.*, 2002). However, the dependency on other sensors and the exclusion of frequency bands which may include low modal frequencies of the structure (e.g., in long-span bridges) are rendering such techniques less effective or usable.

In the last decades, the SNR variations due to multipath effect and the satellite motion have been used in GNSS - reflectometry for remote sensing (Chew *et al.*, 2014; Löfgren, Haas and Scherneck, 2014; Roussel *et al.*, 2016) and multipath mapping (Bilich and Larson, 2007). Also, there are studies on the opportunistic use of the multipath effect for indoor positioning (Meissner, 2014). The SNR data derive from the composite, i.e., direct and reflected, signals. After appropriate filtering to isolate the contribution of the reflected signals, information can be extracted on the nature of the reflecting surface.

In this paper, an attempt has been made to use multipath-induced, motion-generated SNR variations to model antenna oscillatory motions, resembling a typical structural response. By using the SNR, we avoid the redistribution of the multipath error which is inherent in the position solution. Also, since, the SNR pattern is generated by the antenna instead of the satellite motion, the size of the reflectors does not need to be as large. Therefore, this approach could help in the localisation of small reflectors and the detailed mapping of a static or fast-changing multipath environment. Finally, this method does not require long monitoring hours and stable antennae, compared to sidereal filtering (Wang *et al.*, 2017), offering practical advantage for bridge monitoring applications. The proposed technique aims to improve the accuracy and reliability of GNSS for deformation monitoring with a potential value in remote sensing.

II. SNR AND CARRIER PHASE MULTIPATH

When multipath is present, one or more reflected signals interfere with the direct signal. The resulted composite signal strength varies as the antenna oscillates, due to the constructive and destructive multipath variations, introducing an oscillatory pattern in the SNR time series. Since the SNR is a function of the total signal amplitude, we can model these multipath fluctuations as sinusoids (Axelrad, Comp and Macdoran, 1996; Bilich, Larson and Axelrad, 2008):

$$SNR \equiv A_c = A_m \cos \psi + A_d \quad (1)$$

where A_c is the composite signal amplitude.
 A_m is the reflected signal amplitude.
 A_d is the direct signal amplitude.
 ψ is the multipath relative phase.

Furthermore, the multipath relative phase, can be derived from the path delay (Roussel *et al.*, 2016):

$$\psi = \frac{2\pi}{\lambda} \delta_i = \frac{2\pi}{\lambda} 2H_i \sin(\beta_i) \quad (2)$$

where λ signal wavelength.

δ is the additional path length of the reflected signal with respect to the direct at time i .

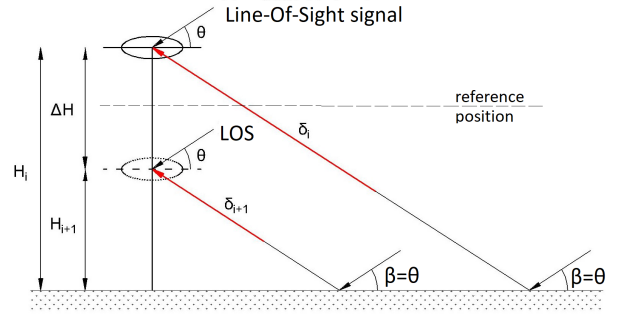


Figure 1. Geometry of ground reflections for a vertically oscillating antenna on two consecutive instances. The ground is assumed flat ($\gamma = 0$) and homogeneous.

H is the antenna - reflector vertical distance at time i .

β is the incidence angle of the reflected signal at time i .

The incidence angle of the reflected signal can be expressed as:

$$\beta = \theta - \gamma \quad (3)$$

where θ is the satellite elevation angle.

γ is the reflector inclination angle.

There is an extended literature on the relationship between SNR and carrier phase multipath (Lau and Cross, 2006) in the case of a stable GNSS antenna (e.g., permanent GNSS stations). However, the same approach can also be applied to an oscillating antenna and a stationary reflector. When the antenna oscillates vertically (Figure 1), the reflection point, also, oscillates with the same frequency across the reflecting surface, e.g., the ground. For short periods of antenna motion (e.g., < 1 min), the satellite elevation angle (θ) and the reflector inclination angle (γ) can be assumed quasi-constant or slowly varying quantities compared to the antenna motion speed. The antenna oscillatory motion is, therefore, the major contributor to the antenna-reflector vertical distance variations (ΔH) and, subsequently, to the multipath relative phase variations ($\Delta\psi$). By adapting Equation (2), these variations can be expressed as:

$$\Delta\psi = \frac{2\pi}{\lambda} (\delta_{i+1} - \delta_i) = \frac{2\pi}{\lambda} 2\Delta H \sin(\beta) \quad (4)$$

For a vertically oscillating antenna and ground reflection, the antenna-reflector distance at any given time t_i is equivalent to the antenna height which can be modeled as:

$$H_i = H_0 + A_{mot} \sin \omega t_i \quad (5)$$

Where H_0 is the antenna height at the reference position.

A_{mot} is the antenna motion amplitude.

$\omega = 2\pi f$ is the angular frequency of motion.

f is the antenna motion frequency.

From Equations (1) - (5), a set of parameters defining the SNR variations can be extracted, which includes: the direct signal amplitude A_d , the reflected signal amplitude A_m , the satellite elevation angle (θ), the reflector inclination angle γ and the antenna – reflector perpendicular distance H , which includes the nominal antenna-reflector distance H_0 , the antenna oscillation amplitude A_{mot} and frequency f .

Depending on the application, different unknowns need to be estimated. For instance, in structural monitoring applications, where the focus is on the characteristics of the structure response, the antenna oscillation amplitude A_{mot} and frequency f are the main parameters to be estimated, or needed, whereas, in remote sensing applications, where a pre-defined antenna motion can be applied, the reflected to direct signal amplitude A_m/A_d , the reflector inclination angle γ and the nominal antenna - reflector distance H_0 are the parameters of interest.

III. SNR BASED MOTION DETERMINATION

A. Experiments description

A series of simulations using the GSS8000 Spirent simulator was undertaken, where the antenna was subjected to a vertical oscillation with a range of amplitudes between 5 mm and 4 cm and frequencies between 0.1 Hz and 2 Hz. The simplified model of specular ground multipath was used, where the ground is simulated as a homogeneous horizontal surface 1.6 m under the antenna phase centre, generating one reflected signal per satellite. A Javad Triumph-1 receiver was used to collect the simulated data. Experiments were conducted with ground reflected signals attenuated by 10 dB, 20 dB and 30 dB with respect to the direct signal strength. The amplitude and frequency of the antenna motion were imported in the simulated scenario as an NMEA (National Marine Electronics Association) - formatted file in a 20 Hz sampling rate and the same values were used to form the analytical solution. The direct signal strength used in the analytical solution, in Equation (1), is equal to the mean SNR level generated in a simulated multipath-free environment. The satellite elevation angles were extracted from the RINEX navigation file output from the simulation.

More than 50 different combinations of antenna motion and ground reflection attenuation were simulated with and without enabling an antenna radiation pattern and atmospheric model.

Figure 2 presents an indicative segment of the SNR time series for satellite PRN 11 on a multipath-free and ground multipath simulated environment. The antenna was subjected to a series of one-minute vertical oscillations. In a multipath-free environment, the SNR maintains an approximately constant average value and the potential variations reflect only the noise produced by the simulator and receiver. The multipath contaminated SNR time series consists of two

superimposed patterns; a slow varying sinusoidal

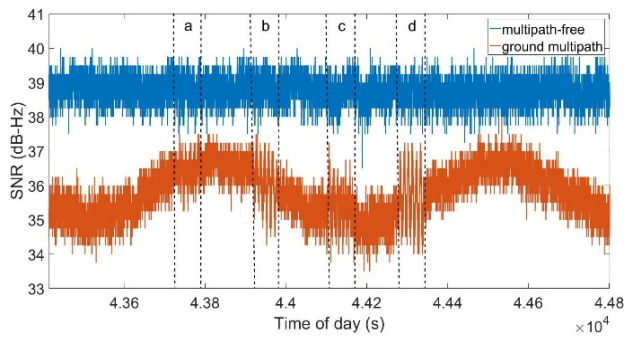


Figure 2. SNR time series for PRN 11 in a multipath – free (blue) and ground multipath (red) simulated environment. The antenna motion intervals correspond to vertical oscillations of 0.1 Hz with amplitudes of (a) 1 cm, (b) 2 cm, (c) 3 cm and (d) 4 cm. The multipath-free SNR time series have been offset for clarity.

pattern due to the satellite elevation angle change, while the satellite moves along its orbit, and regular intervals of high-frequency variations corresponding to the antenna vertical oscillation intervals. These motion-generated variations have the same frequency with the antenna motion and are caused by the change of the perpendicular distance between the antenna and the reflector, i.e. the ground, as a function of the antenna height.

The ratio of the direct to reflected signal amplitude α , depends on the ground reflection attenuation and the antenna radiation pattern, and its value is computed according to the formula employed by the receiver to measure the signal strength. Therefore, the value of this parameter cannot be analytically estimated, and it is receiver-dependent. However, given a defined simulated multipath environment, as the specular ground multipath described here, and absence of an antenna radiation pattern, the parameter α is, theoretically, expected to be the same for all satellites and antenna motion types. The noise embedded in the SNR data, and the SNR resolution can partially mask or distort the motion - generated pattern in the SNR time series and induce variations in the computed value of the parameter α for the same simulated multipath conditions. The magnitude of these variations defines the goodness of fit of the analytical solution to the simulated and, subsequently, the accuracy of the antenna motion estimation.

The validation of the analytical solution is implemented using the following procedure.

1. The multipath relative phase for each trial is constructed from Equation (2) using the known values for the satellite elevation angle, the signal wavelength, the reflector inclination angle (0° in all experiments), the antenna-reflector vertical distance (1.6 m in all experiments) and the antenna motion amplitude and frequency.
2. The customised function in Equation (1) is fit into the simulated SNR for each trial by creating a custom nonlinear model and using the nonlinear

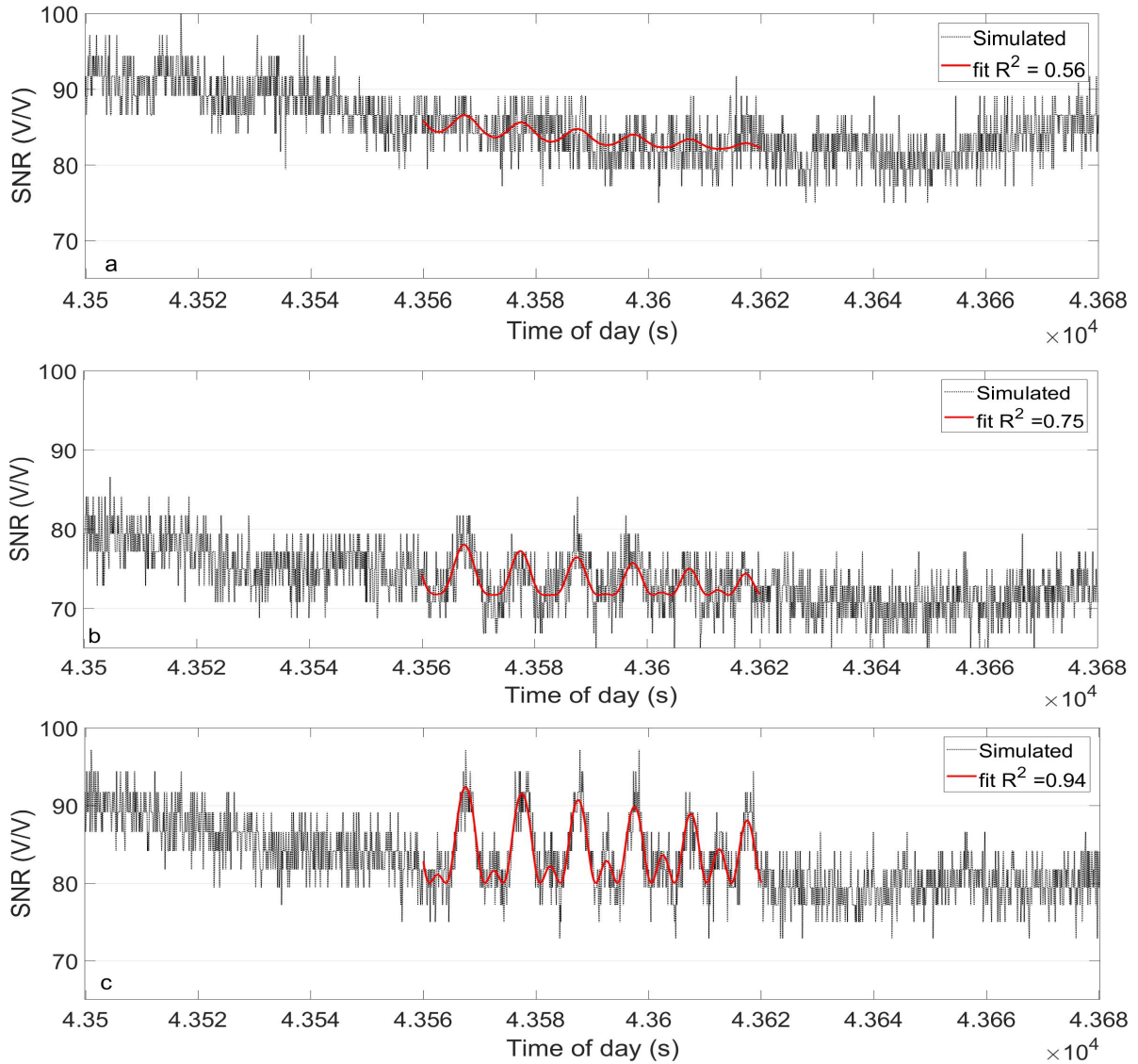


Figure 3. Fit of the simulated SNR using the customised function as shown in step 2 of the procedure. The plots are for PRN01, motion frequency 0.1 Hz and motion amplitude (a) 5 mm, (b) 20 mm and (c) 40 mm.

least squares method from the MatLab Curve fitting Toolbox¹ to estimate the reflected signal amplitude, A_m , and the direct signal amplitude, A_d .

3. The estimated parameter A_m is checked for consistency under the various cases of antenna motion and the goodness of fit. The fixed signal reflection attenuation is expected to yield a constant value on the parameter A_m . The consistency and accuracy of the A_m value indicates the robust relationship between the antenna motion and the generated SNR pattern under various types of antenna motion and the goodness of fit indicates the effect of the hardware noise on the motion-generated SNR pattern.

B. The effect of antenna motion on SNR

Figure 3 shows the SNR time series and the nonlinear least squares fit for different antenna motion amplitudes and frequencies. For small motion amplitudes, the SNR variations are small and partially masked from the SNR time series noise. Also, the large data spread for small motion amplitudes is reflected in the low coefficient of determination (R^2) of the fit. Finally, it should be noted that the peak-to-peak amplitude variations in the resulting SNR pattern during the 60 min interval, shown in Figure 3, are induced by the contribution of the satellite elevation angle changes in the resulting SNR.

C. The effect of multipath intensity on SNR

This series of trials investigate the SNR behaviour under various antenna motion amplitudes ranging from

1

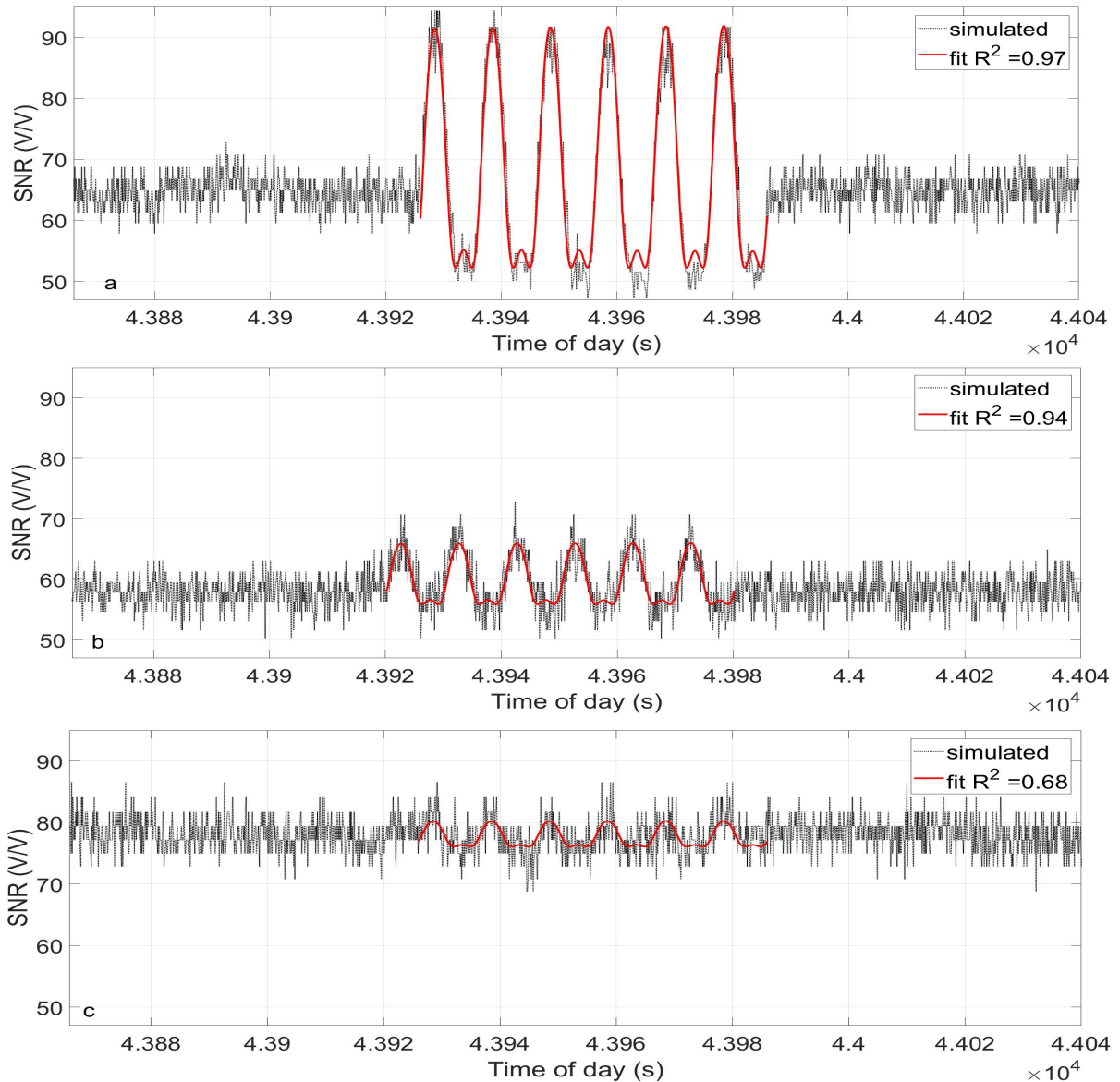


Figure 4. Fit of the simulated SNR with respect to the constructed multipath relative phase using the customised function as shown in step 2 of the procedure and the corresponding time series. The plots are for PRN08, motion frequency 0.1 Hz, motion amplitude 20 mm and reflection attenuation (a) 10 dB, (b) 20 dB and (c) 30 dB.

5 to 40 mm with a constant motion frequency of 0.1 Hz in three cases of reflection attenuation, at 10 dB, 20 dB and 30 dB. The analysis includes the same satellites and intervals of orbits as Section B. The trials were performed in order for the satellites to be at the same elevation angle for constant motion amplitude and varying reflection attenuation. As can be seen from Equation (1) and observed in Figure 4, the SNR amplitude is proportional to the reflected signal amplitude A_m . Thus, the stronger the reflection attenuation the smaller is the SNR amplitude. Concerning the goodness of fit, we see that for 10 dB, 20 dB and 30 dB reflection attenuation the R^2 is 0.97, 0.94 and 0.68, respectively, which is expected as the magnitude of the motion-generated SNR pattern is proportional to the multipath interference.

D. The effect of antenna radiation pattern on SNR

This series of trials investigates the effect of the antenna radiation pattern on the motion - generated SNR pattern. The analysis includes the GPS satellite PRN 25 in a 4h-orbit at an elevation from 0° to 70° . The type of motion used in 1-min intervals during the orbit of the satellite has an amplitude of 30 cm and frequency 0.1 Hz. The ground reflection attenuation, i.e., the attenuation of the reflected signal from the bouncing off the ground, is set to 20 dB for the whole duration of the simulation. The antenna radiation pattern inserted in the simulator resembles the Leica AS 10 pattern, as this antenna type was used in field experiments and is a typical geodetic antenna.

Figure 5 shows the SNR time series with respect to the satellite elevation angle for PRN 25 with the two distinguished types of multipath induced effect: (i) the slow varying pattern corresponding to the multipath

geometry changes due to the satellite motion and, (ii) the fast-varying intermittent pattern corresponding to the intervals of antenna oscillatory motion. Both effects are more intense in low satellite elevation angles, getting subtler and finally disappearing in high elevation angles when the reflections are suppressed by the antenna radiation pattern. Also, the antenna radiation pattern effect on the signal amplitude variations due to changes in the antenna orientation seems to be negligible contributor compared to the carrier phase multipath interference on the resulting SNR pattern, for small oscillation amplitudes, e.g. typical structural vibrations.

The analysis of all the trials was implemented following the procedure in Section III-A, setting two more parameters as unknowns, in addition to the direct and reflected signal amplitude; the antenna - reflector vertical distance, H_0 , and the motion amplitude A_{mot} . By fitting the custom function (Equation 1) to the SNR time series we acquire the values of the 4 unknowns.

The analysis yielded the direct and reflected signal amplitude results shown in Figure 6. As the satellite rises the direct signal amplitude increases and the reflected signal amplitude decreases in a linear trend as the antenna radiation pattern amplifies the direct signal (positive angle of arrival) and suppresses the reflected (negative angle of arrival). The motion amplitude is correctly estimated in most of the trials corresponding to satellite elevations below 58° (Figure 7). Although all three unknowns converged to the correct values in most trials, the antenna - reflector vertical distance

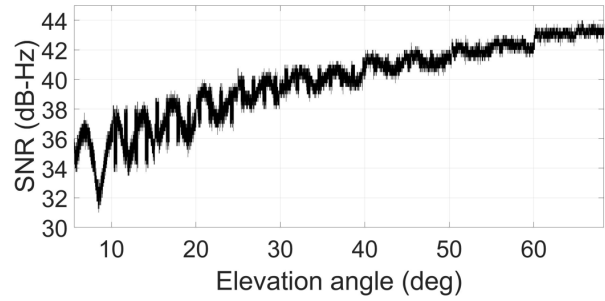


Figure 5. SNR time series for PRN25.

estimation did not converge to the correct value 1.6 m and rather varied in a random way. This is due to the fact that the SNR amplitude is very sensitive to the antenna-reflector distance, and small differences of the latter, in the order of a few centimetres, can yield different SNR amplitudes. Although this sensitivity enables the cm-level estimation of the antenna-reflector distance, if the SNR amplitude is accurately modelled, it impedes the proper convergence of the model to the correct value. Also, there are cases of multiple values yielding the same SNR amplitude for a given motion amplitude A_{mot} and incidence angle β . The application of boundary conditions, e.g., by using Fresnel zones (Zimmermann *et al.*, 2019), could lead the convergence to the correct values; however this requires the observation of the multipath environment in a case-by-case basis.

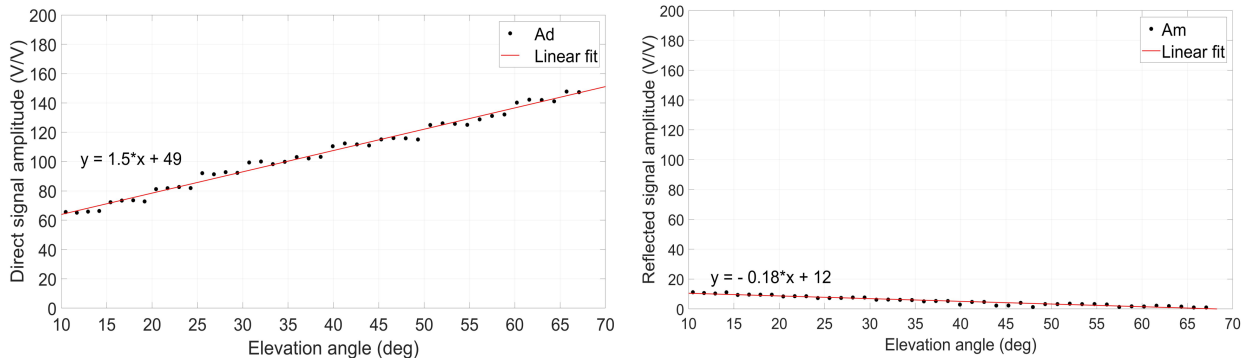


Figure 6. (Left) direct and (right) reflected signal amplitude estimation with respect to the satellite elevation angle for PRN 25.

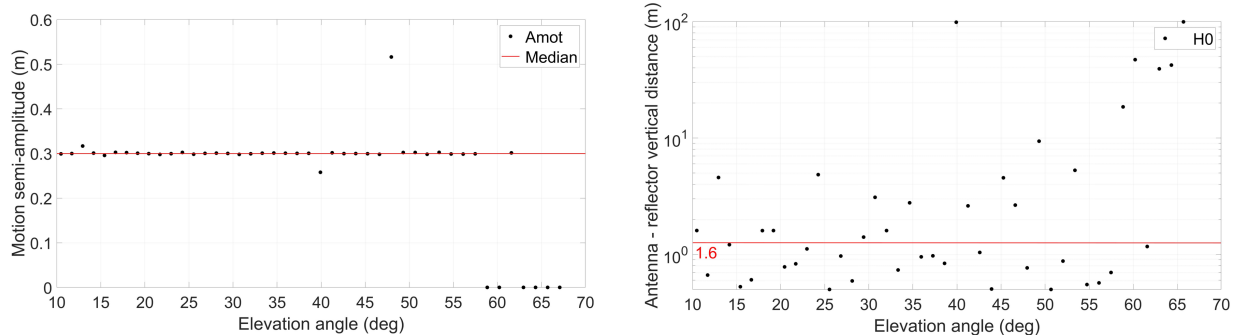


Figure 7. (Left) antenna motion amplitude and (right) antenna-reflector vertical distance estimation with respect to the satellite elevation angle.

IV. FIELD EXPERIMENTS AND RESULTS

A. Experiments description

A series of experiments were carried out at the roof of the Nottingham Geospatial Building with a vertically moving antenna at different amplitudes and frequencies of oscillation. A GNSS station consisted of a Leica GS 10 receiver recording at 10 Hz and an AS 10 antenna installed on a heavy-duty tripod, where the height was adjustable using a manually rotating handle. Additionally, a Robotic Total Station (RTS) was recording the motion with a sampling rate capacity of 10 Hz, using a 360° prism mounted on the tripod below the GNSS antenna. The height of the antenna phase centre was 1.6 m from the ground.

The excitations were executed, emulating dynamic and semi-static motion, which are the main types of the response of civil engineering structures. The GNSS antenna was subjected to various amplitudes and frequencies of vertical motion, ranging between 0.4 and 4.5 cm and between 0.007 and 1 Hz, respectively, depending on the type of excitation. More details on the experiment can be found in (Peppas, Psimoulis and Meng, 2017).

The same series of experiments were conducted using a Samsung Galaxy S8 mounted on the heavy-duty tripod and recording the SNR of the satellite signals.

B. Discussion

Figure 8 shows the SNR for PRN 10 and GPS displacement time series for antenna motion with 8 mm amplitude and 0.3 Hz frequency using an AS10 antenna.

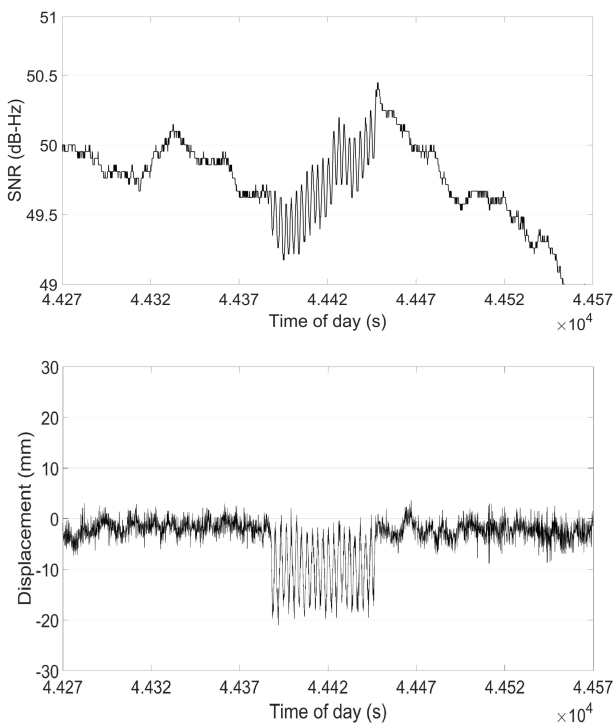


Figure 8. SNR for PRN10 and GPS displacement time series during antenna motion of 16 mm peak-to-peak amplitude and 0.3 Hz frequency.

Figure 9 shows the SNR time series for PRN 08, as recorded by the mobile phone for similar motion amplitudes and frequencies to the experiment with the AS10 antenna. It should be noted the difference of one

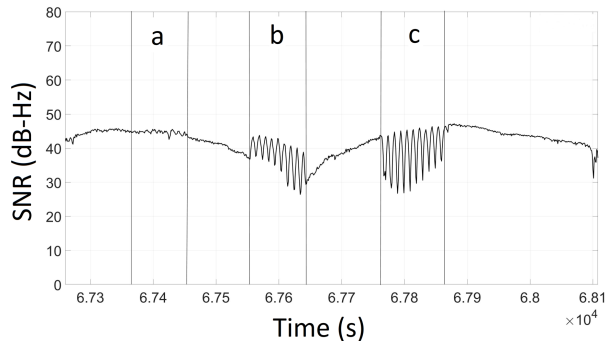


Figure 9. SNR time series of PRN08, as recorded by Samsung Galaxy S8, for (a) 7.5 mm, (b) 15 mm and (c) 30 mm amplitude of antenna motion at 0.1 Hz.

order of magnitude between the SNR amplitude variations in the two cases. The chip antenna is more susceptible to multipath compared to the geodetic antenna. Thus, the multipath geometry changes generated by the antenna motion have a more profound effect on the SNR time series.

The multipath sensitivity of low-cost antennae can be an asset for reflectometry and, therefore, counterbalance the poor positioning accuracy.

This paper investigates, analytically and using simulations, the case of one reflector per satellite causing specular reflections. In real conditions, it is logical to assume that a clear consistent SNR pattern could only be induced by a unique dominant reflector. Therefore, the one-reflector model seems to be adequate to represent a real case without the need for more complex multipath models with many reflectors and multiple reflection paths. However, extensive study is needed on whether the antenna motion characteristics can be extracted from the SNR time series.

V. CONCLUSIONS

In this study, the potential of modelling the GNSS antenna vibrations is investigated by analysing the SNR signature due to the carrier phase multipath. The proposed approach is based on the known method of modelling the multipath for static GNSS antennae in remote-sensing applications. However, in this study, we inverse the conditions by having a static multipath environment and an oscillating GNSS antenna.

The dynamic multipath effect, due to the antenna motion, on the SNR time series has been successfully modelled through GNSS simulations. The analysis of the simulations revealed the impact of the different parameters of multipath and the difficulty of modelling the distance between the GNSS antenna and the reflector.

The performance of the model and its convergence to reliable estimations of the multipath parameters will be

benefited by the application of boundary conditions and constraints, which limits the possible solutions and leads to faster and more accurate results. This is essential in cases where the multipath and antenna vibration parameters are considered unknown.

The preliminary analysis of experimental GNSS data shows that the impact of multipath is more clearly reflected in the SNR time series for low-cost antennae (e.g., smartphones). Therefore, this approach could be conjointly used to augment the resulted positioning accuracy and availability increasing, for instance, the capabilities of mobile phones in deformation monitoring applications as an alternative to hardware mitigation techniques for low-cost monitoring systems (Zhang and Schwieger, 2017). Another approach could be the generation of code and carrier phase corrections from determination of the multipath parameters leading to improvement in the position solution.

However, further analysis of the experimental data is needed to shed more light in the efficient modelling and parameter estimation in real conditions.

VI. ACKNOWLEDGEMENTS

The authors would like to thank Dr Lukasz Bonenberg who contributed to the experimental measurements. This article benefited from constructive comments of two anonymous reviewers.

References

- Axelrad, P., Comp, C. J. and Macdorran, P. F. (1996) 'SNR-Based Multipath Error Correction for GPS Differential Phase', 32(2).
- Bilich, A. and Larson, K. M. (2007) 'Mapping the GPS multipath environment using the signal-to-noise ratio (SNR)', *Radio Science*, p. RS6003.
- Bilich, A., Larson, K. M. and Axelrad, P. (2008) 'Modeling GPS phase multipath with SNR : Case study from the Salar de Uyuni , Bolivia', *Journal of Geophysical Research*, 113, p. B04401.
- Chew, C. C. *et al.* (2014) 'Effects of near-surface soil moisture on GPS SNR data: Development of a retrieval algorithm for soil moisture', *IEEE Transactions on Geoscience and Remote Sensing*, 52(1), pp. 537–543.
- Lau, L. and Cross, P. (2006) 'A new signal-to-noise ratio based stochastic model for GNSS high-precision carrier phase data processing algorithms in the presence of multipath errors', in *Proc. 19th Int. Tech. Meet. Satell. Div. Inst. Navig.* Fort Worth, TX, pp. 276–285.
- Lau, L. and Cross, P. (2007) 'Investigations into Phase Multipath Mitigation Techniques for High Precision Positioning in Difficult Environments', *The Journal of Navigation*, 60(3), pp. 457–482.
- Li, X. *et al.* (2006) 'Full-scale structural monitoring using an integrated GPS and accelerometer system', *GPS Solutions*, 10(4), pp. 233–247.
- Löfgren, J. S., Haas, R. and Scherneck, H. G. (2014) 'Sea level time series and ocean tide analysis from multipath signals at five GPS sites in different parts of the world', *Journal of Geodynamics*, 80, pp. 66–80.
- Meissner, P. (2014) *Multipath-Assisted Indoor Positioning*, Graz University of Technology.
- Meng, X., Dodson, A. H. and Roberts, G. W. (2007) 'Detecting bridge dynamics with GPS and triaxial accelerometers', *Engineering Structures*, 29(11), pp. 3178–3184.
- Moschas, F., Psimoulis, P. A. and Stiros, S. C. (2013) 'GPS / RTS data fusion to overcome signal deficiencies in certain bridge dynamic monitoring projects', *Smart Structures and Systems*, 12(3–4), pp. 251–269.
- Moschas, F. and Stiros, S. (2011) 'Measurement of the dynamic displacements and of the modal frequencies of a short-span pedestrian bridge using GPS and an accelerometer', *Engineering Structures*, 33(1), pp. 10–17.
- Peppas, I., Psimoulis, P. and Meng, X. (2017) 'Using the signal-to-noise ratio of GPS records to detect motion of structures', *Structural Control and Health Monitoring*, (February), p. e2080.
- Psimoulis, P. *et al.* (2015) 'Consistency of PPP GPS and strong-motion records: case study of Mw9.0 Tohoku-Oki 2011 earthquake', *Smart Structures and Systems*, 16(2), pp. 347–366.
- Roberts, G. W. *et al.* (2002) 'Multipath Mitigation for Bridge Deformation Monitoring', *Journal of Global Positioning Systems*, 1(1), pp. 25–33.
- Roussel, N. *et al.* (2016) 'Detection of Soil Moisture Variations Using GPS and GLONASS SNR Data for Elevation Angles Ranging From 2° to 70°', *IEEE Journal of Selected Topics in Applied Earth Observations and Remote Sensing*, 9(10), pp. 4781–4794.
- Strode, P. R. R. and Groves, P. D. (2016) 'GNSS multipath detection using three-frequency signal-to-noise measurements', *GPS Solutions*, 20(3), pp. 399–412.
- Wang, D. *et al.* (2017) 'Multipath extraction and mitigation for bridge deformation monitoring using a single-difference model', *Advances in Space Research*, 60(12), pp. 2882–2895. doi: 10.1016/j.asr.2017.01.007.
- Zhang, L. and Schwieger, V. (2017) 'Investigation of a L1-optimized Choke Ring Ground Plane for a Low-Cost GPS Receiver-System', *Journal of Applied Geodesy*, 12(1).
- Zimmermann, F. *et al.* (2019) 'GPS Multipath Analysis Using Fresnel Zones', *Sensors (Basel)*, 19(1), pp. 1–25.